Journal of Pain Research

Dovepress
open access to scientific and medical research

Open Access Full Text Article

ORIGINAL RESEARCH

Ovine model of neuropathic pain for assessing mechanisms of spinal cord stimulation therapy via dorsal horn recordings, von Frey filaments, and gait analysis

Chandan G Reddy[1]
John W Miller[1]
Kingsley O Abode-Iyamah[1]
Sina Safayi[2]
Saul Wilson[1]
Brian D Dalm[1]
Douglas C Fredericks[3]
George T Gillies[4]
Matthew A Howard III[1]
Timothy J Brennan[5]

[1]Department of Neurosurgery, University of Iowa Carver College of Medicine, Iowa City, IA, USA; [2]Department of Veterinary Clinical Sciences, Iowa State University, Ames, IA, USA; [3]Department of Orthopedics and Rehabilitation, University of Iowa Carver College of Medicine, Iowa City, IA, USA; [4]Department of Mechanical and Aerospace Engineering, University of Virginia, Charlottesville, VA, USA; [5]Department of Anesthesia, University of Iowa Carver College of Medicine, Iowa City, IA, USA

Background: It is becoming increasingly important to understand the mechanisms of spinal cord stimulation (SCS) in alleviating neuropathic pain as novel stimulation paradigms arise.
Purpose: Additionally, the small anatomic scale of current SCS animal models is a barrier to more translational research.
Methods: Using chronic constriction injury (CCI) of the common peroneal nerve (CPN) in sheep (ovine), we have created a chronic model of neuropathic pain that avoids motor deficits present in prior large animal models. This large animal model has allowed us to implant clinical grade SCS hardware, which enables both acute and chronic testing using von Frey filament thresholds and gait analysis. Furthermore, the larger anatomic scale of the sheep allows for simultaneous single-unit recordings from the dorsal horn and SCS with minimal electrical artifact.
Results: Detectable tactile hypersensitivity occurred 21 days after nerve injury, with preliminary indications that chronic SCS may reverse it in the painful limb. Gait analysis revealed no hoof drop in the CCI model. Single neurons were identified and discriminated in the dorsal horn, and their activity was modulated via SCS. Unlike previous large animal models that employed a complete transection of the nerve, no motor deficit was observed in the sheep with CCI.
Conclusion: To our knowledge, this is the first reported large animal model of chronic neuropathic pain which facilitates the study of both acute and chronic SCS using complementary behavioral and electrophysiologic measures. As demonstrated by our successful establishment of these techniques, an ovine model of neuropathic pain is suitable for testing the mechanisms of SCS.
Keywords: neuropathic pain, sheep models, gait analysis, spinal cord stimulation, unit recordings

Introduction

Chronic pain, and neuropathic pain in particular, is a significant public health burden, affecting up to 100 million US adults, costing up to $635 billion each year in medical treatment. A small fraction of these patients fail conservative measures and require interventional procedures such as spinal cord stimulation (SCS).[1] The mechanisms underlying SCS are not well understood.[2]

While current tonic SCS parameters for neuropathic pain are effective,[3] there remain patients whose pain cannot be controlled using existing technology. In response to these failures, newer stimulation parameters have been developed, including high-frequency[4] and burst stimulation,[5] with superior clinical relief of back and leg pain. Unlike tonic SCS, these stimulation paradigms have clinically afforded patients pain relief without paresthesias. Less well understood, however, are the mechanisms by

Correspondence: Chandan G Reddy
Department of Neurosurgery, University of Iowa Hospitals and Clinics, 1849 John Papajohn Pavilion, 200 Hawkins Drive, Iowa City, IA 52242-1086, USA
Tel +1 319 356 2598
Email chandan-reddy@uiowa.edu

submit your manuscript | www.dovepress.com
Dovepress
http://dx.doi.org/10.2147/JPR.S139843

which these alternate stimulation paradigms have accomplished this pain relief.[6] Several hypotheses for biochemical and neurophysiological mechanisms of action are under study, however, including ectopic activity in Aβ-fibers and modulation of dendritic currents, among others.[6]

One reason for this paucity of knowledge is the limited availability of large animal models of neuropathic pain that are suitable for testing and evaluating the hypothetical mechanisms of SCS. Our goal here is to introduce an ovine model capable of meeting this need and to present preliminary data demonstrating the feasibility of using it to assess the effects of SCS on behavioral and electrophysiologic measures of neuropathic pain.

Mechanisms of SCS contributing to the alleviation of pain have been studied extensively in small animal rodent models by recording from dorsal horn neurons (DHNs).[2,7–10] Chronic neuropathic pain as a result of chronic constriction injury (CCI) of peripheral nerves is a well-established model of neuropathic pain in small animals.[11–15] These small animal models have led to the hypothesis that SCS suppresses the activity of wide dynamic range (WDR) neurons in the dorsal horn.[7,8,10] Small animal rodent models, however, have physical limitations in contrast to human and large animal models, in that a small animal model is typically incapable of supporting chronic implantation of large clinical-scale stimulator leads or pulse generators. Additionally, neuronal recordings are more susceptible to electrical artifact during simultaneous SCS due to the smaller anatomic space.

A large animal ovine model of neuropathic pain was recently developed for testing intrathecal drug infusions,[16] a caprine model has been used to test the neurotoxicity of novel SCS stimulation parameters,[17] and a porcine model of neuropathic pain from sciatic nerve ligation has been introduced for testing the efficacy of analgesics.[18] In the ovine model described by Wilkes et al,[16] the common peroneal nerve (CPN) was completely transected. While this model produced the desired neuropathic pain, it also led to a motor deficit in the form of a hoof drop, that is, hoof depression during dorsiflexion while walking, which might limit the utility of any gait analysis employed for assessment. Our goal was to modify the method described by Wilkes et al, adapting the CCI typically used in smaller animals to the ovine model. By constricting the CPN without completely transecting it, we hoped to produce neuropathic pain while avoiding motor deficit.

DHN single-unit recording techniques have been an established technique for many years.[19,20] We adapted Herrero et al's[19] techniques for recording single units from the sheep spinal cord in order to quantitatively measure the manifestation of neuropathic pain reflected in the neuronal activity of the dorsal horn. As previously mentioned, the large scale of the sheep also enables simultaneous recording and stimulation with minimal artifact. This is an opportunity unique to the larger animal model that may enable further insight into the mechanisms of various SCS paradigms.

Therefore, the purpose here is to explore the possibility of introducing a large animal, chronic neuropathic pain model that might enable the study of the effects of SCS via both behavioral and electrophysiologic measures. Our particular model is for pain of peripheral origin, as opposed to that of central origin (e.g., that due to stroke, and so on). By constricting the CPN in the sheep, we have modified a previous model of nerve transection in order to establish a model without motor deficit. Behavioral measures of von Frey filament thresholds and gait analysis, combined with the electrophysiologic measures of dorsal horn recordings, are then conducted both with and without different paradigms of SCS. It is important to note that because of the exploratory nature of this pilot study, we intentionally chose to forego the inclusion of sham experimental procedures. While recognizing that doing so inevitably limits the scope of conclusions that can be drawn, the immediate goal was to simply explore the feasibility of the proposed approach and, if promising, suggest a path forward for future work aimed at a more rigorous evaluation. The techniques developed here can be used to address questions about the mechanisms underlying SCS in a neuropathic pain state, with the ultimate goal of translating these studies to improve pain relief in clinical populations.

Highlights

- Peroneal nerve constriction in sheep produces a reproducible large animal model of persistent neuropathic pain.
- This approach avoids neurologic deficits in gait that otherwise result from complete sectioning of the nerve.
- Single-unit dorsal horn recordings can be used to investigate neural response to SCS therapy.
- Behavioral measures (von Frey filament response and gait analysis) provide independent assessment of SCS effects.

Materials and methods

Overall experimental strategy

Sheep were acclimated to treadmill walking and von Frey filament testing for at least 3 weeks prior to surgical nerve injury and stimulator implant. At the time of peroneal nerve surgery, a spinal cord stimulator lead was inserted via laminectomy at vertebral body L2 along with an implantable, rechargeable pulse generator. Behavioral testing was then resumed

to evaluate the development of tactile hypersensitivity and to assess the effects of peroneal nerve surgery on gait. SCS was then performed to assess the effect of neuromodulation on the behavioral measures of von Frey filament thresholds and gait analysis. At a terminal surgery, DHN activity was recorded at the lumbar enlargement both ipsilateral and contralateral to the injury. SCS was then applied both through the implanted pulse generator and with an external stimulator. An overview of the experimental protocol is shown in Figure 1.

Of the eight sheep used in this study, the first three (#40002, #40006, #40007) were utilized to refine the experimental protocol. Sheep #40006 underwent complete transection of the peroneal nerve, whereas the other seven underwent ligation without transection. Sheep #40007 did not undergo SCS and was used for DHN recording only, whereas the remaining seven sheep were used to study the effects of neuromodulation. Sheep #40002 underwent SCS implantation in a delayed fashion (at 6 months after nerve injury), and DHN single unit recordings were made on sheep #40002 at both the initial and terminal surgeries. Both Sheep #40002 and #40006 were kept alive for beyond 1 year's duration to assess the feasibility of SCS and persistence of neuropathic pain beyond 1 year. An optimized and standardized protocol was then implemented for the remaining five sheep (#40014, #40015, #40016, #40021, #40022) as outlined in Figure 1, in which von Frey filament thresholds were measured at 180 days for 1 month duration, then chronic SCS was instituted and von Frey filaments were remeasured for an additional month.

Animal care and use

Institutional approvals for the protocols described below were obtained from the Institutional Animal Care and Use

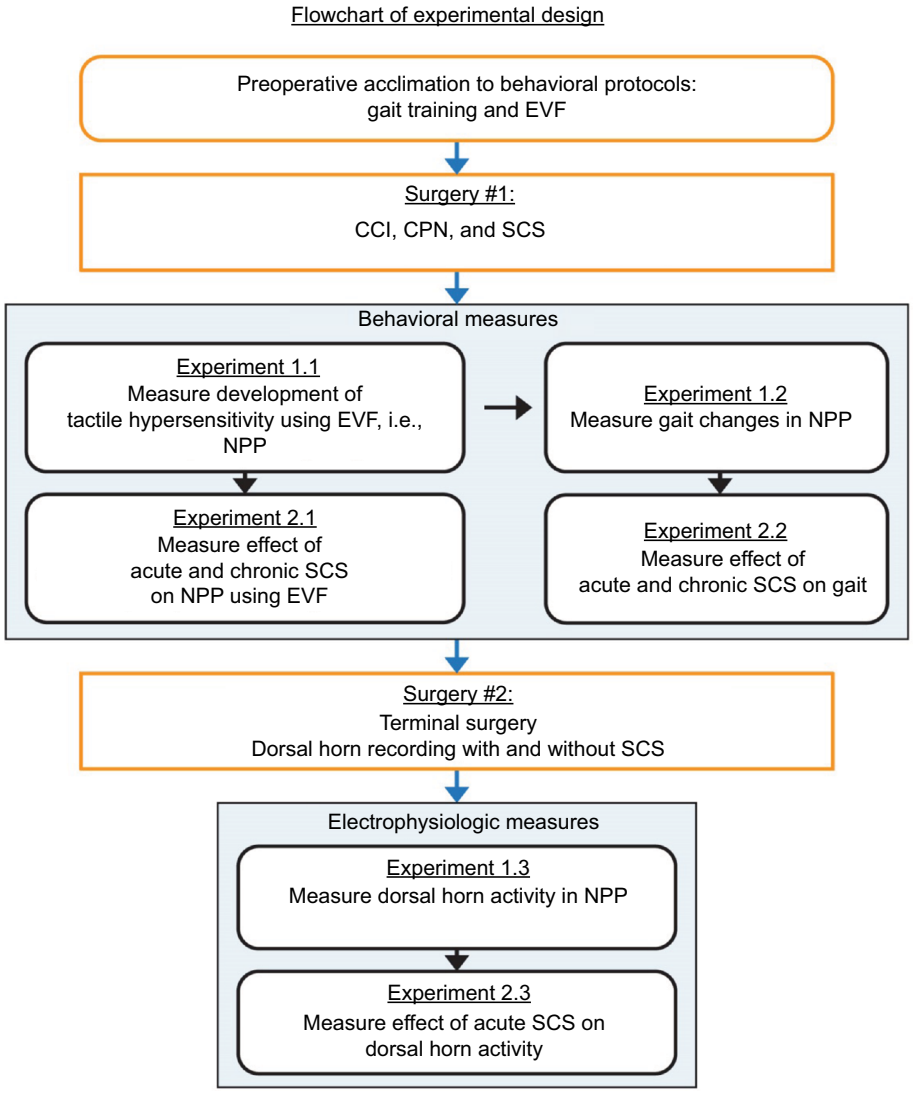

Figure 1 Flowchart showing overview of the protocols for the in vivo ovine studies.
Abbreviations: CCI, chronic constriction injury; CPN, common peroneal nerve; EVF, electronic von Frey filaments; NPP, neuropathic pain; SCS, spinal cord stimulation.

Committees (IACUC) at both the University of Iowa (UI, for the surgical procedures, intraoperative measurements, and behavioral response tests, IACUC approval no. 1308149) and at the Iowa State University (for the gait analysis studies, with and without SCS, IACUC approval no. 2-12-7298-O), which are in accordance with the guidelines of the National Institutes of Health and of the International Association for the Study of Pain. Eight adult female Polypay sheep, ~75 kg each, were used for this pilot study. Female sheep were chosen as they were more docile and acclimated more readily to the testing environment. Upon arrival, the sheep were examined by a veterinarian and deemed nonpregnant and free of disease. After surgery, the sheep were inspected for infection and tested for gross motor deficits by examination of the passive and active motion of the limbs. All experimental animals were maintained under veterinary care in good health.

Surgical method and postoperative care

All surgeries were performed at UI in accordance with the IACUC standards of surgery for large animals. The animals were sedated, and general anesthesia was then induced and maintained with isoflurane delivered in O_2. Each sheep underwent two surgeries. The first surgery involved intervention on the peroneal nerve and placement of a spinal cord stimulator. The second surgery, which was a terminal surgery, included dorsal horn recordings.

Surgery #1: nerve injury and spinal cord stimulator placement

The left peroneal nerve was exposed at the fibular head (Figure 2) as described by Wilkes et al.[16] The nerve was identified just posterior to the stifle joint in close approximation to the fibular head. In one sheep (#40006), the nerve was completely transected, whereas in the remaining seven sheep, a modified CCI was performed with a series of four suture ligatures placed around the nerve, constricting it ~25% as compared to the normal nerve diameter. The modified CCI model was performed to avoid producing motor deficits such as hoof drop or other axotomy-related deficits. This modified CCI approach was designed to follow the original small animal model described by Bennett et al,[21] Bennett and Xie,[22] and Shortland et al.[23] CCI was selected as a departure from the established large animal models to determine whether neuropathic pain could develop without complete sectioning of the nerve.

At the time of CCI, an L3–4 laminectomy was also performed for insertion of a spinal cord stimulator with final positioning at the L2–3 vertebral segments. A conventional paddle-type epidural spinal cord stimulator (Specify™ 5-6-5 Model 39565; Medtronic Inc., Minneapolis, MN, USA) with a rechargeable subcutaneous battery (RestoreUltra® Model 37712, Medtronic Inc.) was implanted.

All sheep recovered postoperatively without adverse events. Von Frey thresholds were determined over the subsequent 30 days to document the development of tactile hypersensitivity. All the animals were then transferred to the Iowa State University for gait analysis.

Surgery #2: dorsal horn recordings

This terminal surgery was performed under general anesthesia with isoflurane. An L5–6 laminectomy was performed to expose the thecal sac over the lumbar enlargement, the region of the spinal cord receiving input from the CPN. The recording tower for the microelectrode system (details provided in the "Dorsal horn recording system" section; Figure 3) was then secured in place for dorsal horn recordings. These

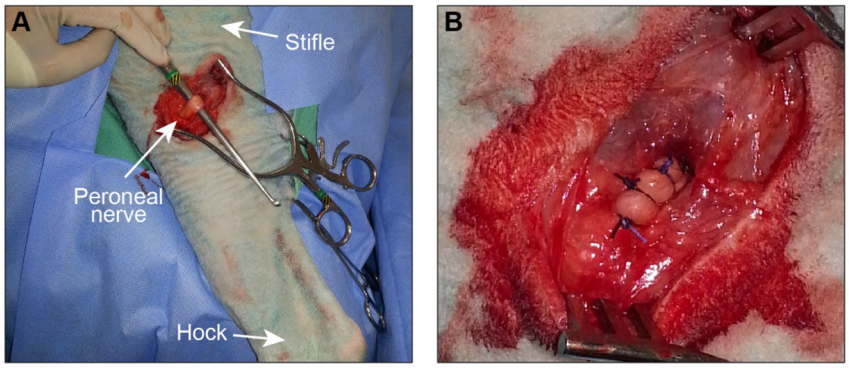

Figure 2 (**A**) Dissection and isolation of the peroneal nerve at the level of the stifle joint. The nerve is palpable just behind the stifle joint, coursing around the fibular head. The stifle and hock joints are marked for reference, in addition to the peroneal nerve. (**B**) Four suture ligatures have been placed around the nerve to create a 25% constriction (i.e., a reduction in the diameter of the constricted nerve from the normal diameter by 25%).

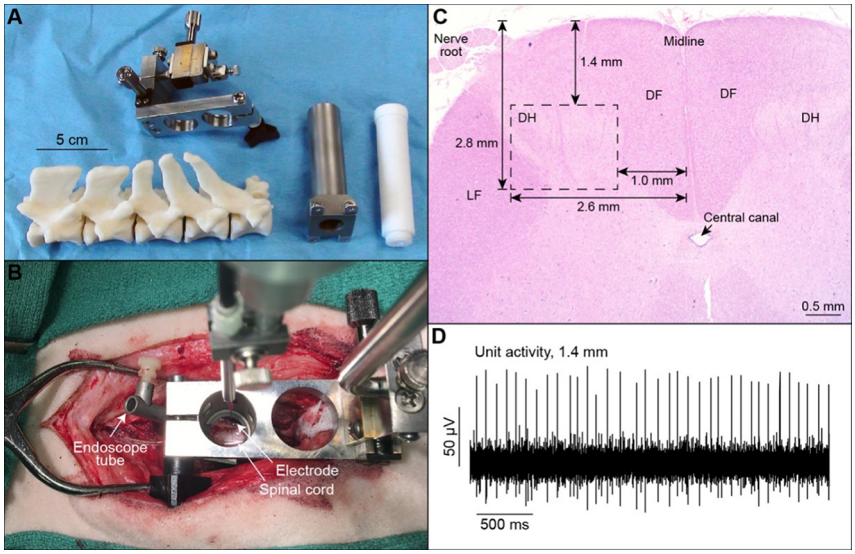

Figure 3 (**A**) Relative to a mock spinal column, from left to right are shown the micrometer-driven translation stage used to control the microelectrode insertion depth and position, the mounting tower, and the Teflon® threaded plug used to seal the tower interior when not in use. (**B**) Top–down view of the apparatus from (**A**) anchored in place on the sheep spinal column for a dorsal horn recording. (**C**) H&E stain of an axial cross section of the dorsal portion of the spinal cord at the level of the lumbar enlargement (L6). The white matter tracts of the spinal cord are slightly more eosinophilic, and the neuron-containing gray matter shows the characteristic butterfly wing structure. The dashed rectangle outlines the targeted recording region within the dorsal horn. The DF, DH, LF, and the central canal are marked. (**D**) Example recording of a single neuron's activity recorded at a depth of 1414 µm.
Abbreviations: DF, dorsal funiculi; DH, dorsal horn; LF, lateral funiculus.

recordings were performed on DHNs both ipsilateral and contralateral to nerve injury. The spinal cord stimulator leads were exposed and dorsal horn recordings were performed as described below. DHNs in the ipsilateral and contralateral sides were characterized during with and without SCS, using tonic, high-frequency, and burst stimulation. After all recordings were completed, the sheep were euthanized.

Behavioral testing methods

All animals were acclimated to behavioral testing using von Frey filament thresholds and treadmill gait training for at least 3 weeks prior to nerve injury.

von Frey studies

Mechanical withdrawal testing was performed to establish mechanical sensitivity, both pre- and post-nerve ligation. Several groups[24–27] have employed variants of this approach to testing limb sensitivity in sheep with neuropathic pain over the past 30 years. To be consistent with the most recent work of this type, we followed the protocol described by Wilkes et al.[16] An electronic anesthesiometer (model 2390; IITC Inc., Life Science Instruments, Woodland Hills, CA, USA) with a stiff von Frey filament tip (max. force 1000 g) was applied to the lateral hind limb in the sural nerve sensory distribution with increasing pressure until hind limb withdrawal. The standard approach was to make three measurements twice each day on each hind limb, 3 days per week (MWF) over the course of one month's duration at a time. These time points included 1 month pre-ligation, 1 month immediately post-ligation, at 180 days (6 months) for 1 month prior to initiation of SCS, and at 7 months for 1 month of concurrent chronic SCS. The median values were recorded, and the order of limb measurement randomized. The force applied at hind limb withdrawal was recorded as the withdrawal threshold.

Treadmill gait analysis

Digital motion capture of the walking patterns of quadrupeds on treadmills, and the subsequent assessment of their limb motions by gait analysis algorithms, provides a sensitive means of investigating degrees of spinal cord injury.[28,29] We have adapted this approach for use with our ovine model and employed it here for assessment of the gait following nerve injury. Gait analysis was performed both with and without SCS.

Each sheep was led onto a treadmill and allowed to stand quietly while acclimating to the laboratory environment. The treadmill belt was then started at a minimal speed that was then increased in small increments until a steady walking rate of ~4.5 km/h was reached.[30] Each acclimation session lasted ~30–45 minutes, which was repeated 6–10 times over 3 weeks for full acclimatization.

The full details of the multi-camera video imaging system and motion analysis package are provided elsewhere.[31,32] The

motion analysis system had six infrared cameras operating at frame rates of 100 Hz (Vicon Motion Systems Ltd., Oxford, UK), which was used to monitor the trajectories of 14 mm diameter optical markers attached noninvasively to the skin near bony landmarks on the pelvic limbs. In particular, the motion of the hock (tarsal/tarsus) joint was defined using three markers attached to tibial and metatarsal regions. There were typically two data recording days for each animal, at midpoints over their involvement in the study. On these days, three to five video sessions of 2 minutes length (about 140 steps on the treadmill) were performed. These were done both with and without SCS. The raw video data obtained during the recording sessions were exported to a Matlab® computational package (version 9.3.0.713579; MathWorks Inc., Natick, MA, USA) for extraction of range of motion, angular velocity, and acceleration of the hock joint. These quantitative measures enabled the height of both back hooves to be calculated throughout the gait cycle.

Electrophysiologic testing methods

Dorsal horn recording system

We adapted the method of Herrero et al[19] to obtain recordings from single neurons in the dorsal horn of the spinal cord of anesthetized sheep. A custom-built recording tower was secured to the vertebra with bone screws after laminectomy at the L5–6 level. The dura was opened by sharp dissection and the spinal cord exposed. A penetrating microelectrode (Model WE30031.0A10; World Precision Instruments, MicroProbes, Gaithersburg, MD, USA) with an impedance of 1.0 MΩ was advanced using micrometer-driven translation stages from the pial surface ventrally through the spinal cord. Microelectrode penetrations within the dorsal horn were guided by a microdrive and micro-positioner (Model 2662; David Kopf Instruments, Tujunga, CA, USA). Recording locations included both the ipsilateral and contralateral sides of the spinal cord at varying distances from the midline. A port fixed to the tip of the custom-built apparatus allowed for endoscopic visualization of the electrode tip from an angle of either zero or 30° (Stryker, Kalamazoo, MI, USA). The components of the apparatus and a typical insertion pattern for obtaining the recordings are shown in Figure 3. Anatomic targeting of the dorsal horn was based on measurements shown in Figure 3C.

Recordings were acquired using a high-impedance headstage and preamplifier (Models HZP and P511; Grass Technologies, Natus Neurology, San Carlos, CA, USA). The resulting signals were band-pass filtered between 300 Hz and 10 kHz, amplified with a gain of 100, and then displayed in real time on an oscilloscope. The data were acquired using a high-bandwidth processor (Tucker Davis Technologies, Alachua, FL, USA) sampling at 24 kHz and stored on a laboratory computer for off-line analysis, with Matlab (MathWorks, Inc., Natick, MA, USA) and Offline Sorter™ (Plexon Inc., Dallas, TX, USA) software.

Dorsal horn recording protocol

Prior to starting each recording block, the electrode depth was reset to 0 μm at the surface of the spinal cord. The electrode was then slowly advanced ventrally into the spinal cord at a rate of 10 μm/step using the hydraulic microdrive until spontaneous neuronal activity (SA) was detected. If a neuron with SA was found, mechanical search stimuli (touch, brushing, pinching, deep pressure, hock flexion, and extension) were then applied throughout the hindlimb to ascertain if the neuron had a receptive field in the limb. If a maximal depth of ~2500 μm was reached before any SA was found, the electrode was then withdrawn slowly (10 μm/step) to the dorsal surface of the spinal cord, and at the same time, mechanical stimuli were applied to the hindlimb to identify any mechanosensitive neurons without SA. We included recordings of neurons with no receptive field but SA.

Once a DHN with a receptive field in the hindlimb was identified, the depth of the recording was noted and the following protocol was employed. Before somatic stimulation, baseline activity of the neuron was recorded for 1 minute. A neuron with SA was defined as having mean activity >0.1 impulse/s over this period. To further characterize the neurons, brush, touch, non-damaging pinch, and deep pressure were applied to the hindlimb, gastrocnemius, and hamstring muscles, followed by flexion and extension of the hock joints. Each stimulus was applied for ~3 s, and the interstimulus interval was 5–10 s unless continued activation persisted longer than this. Any continued increase in action potential firing that lasted >2 s following the cessation of a stimulus was defined as after discharge.

After the DHN was characterized, SCS was applied using conventional, high-frequency, and burst stimulation as detailed below. For 1 minute each, spontaneous dorsal horn activity was recorded during SCS, followed by mechanical stimuli of touch, brush, pinch, deep pressure, and hock flexion/extension. After termination of SCS, the neuron was allowed to recover for 30 s prior to initiation of the next SCS paradigm. The order of SCS paradigms was typically tonic stimulation followed by high-frequency and burst. During some sessions, the implanted pulse generator

was used to assess the difference between electrical artifacts from the internal battery compared to the externalized signal generator (Agilent 33500B; Agilent Technologies, Loveland, CO, USA).

Neurons were classified based on the cutaneous classification scheme.[33] In this study, neurons were classified as WDR or high-threshold (HT) neurons, based on the response to brushing and to pinch. HT neurons were identified as neurons that responded to pinch, but not to brush. WDR neurons responded to brush, touch, and pinch as well, with higher amplitude responses to more intense stimuli. Any low-threshold neurons that responded maximally to brush, but also had the same or smaller response to pinch were excluded from this study. We refer to the neurons as WDR and HT.

Spinal cord stimulation

The effect of SCS was assessed using both behavioral assays (von Frey filaments, treadmill gait) and electrophysiologic recordings (dorsal horn recordings). All stimulation paradigms were charge balanced and used a simple bipolar lead configuration spanning the midline. For all behavioral testing, stimulation was delivered via the implanted pulse generator. After tactile hypersensitivity had developed, the stimulator was activated at a continuous setting (0.1 V, 40 Hz, 120 μs pulse width) that did not appear to cause discomfort or obvious behavioral change in the sheep. The von Frey filament measures were then taken three times daily over the course of a week of chronic stimulation.

Sheep were tested for gait during treadmill sessions with and without spinal cord simulation. A typical recording session consisted of five 2-minute trials with the stimulator set as follows: Off, 0.1, 0.3, 0.5 V, Off. The treadmill was stopped between recordings, while the voltage was changed. All the sheep were then returned to UI for dorsal horn recordings.

For the dorsal horn recordings, SCS was applied using both the implanted pulse generator and the externalized signal generator (Agilent 33500B, Agilent Technologies). The externalized signal generator allowed for nonconventional stimulation paradigms of high frequency (10 kHz, 30 μs pulse width, biphasic waveform, 1 V) and burst (500 Hz, 1000 μs pulse width, biphasic waveform applied over 10 ms with a 15 ms interpulse interval, 0.25–0.5 V), as per De Ridder et al,[34] in addition to the conventional tonic stimulation setting (40 Hz, 120 μs pulse width, 1 V). When the implanted pulse generator was used for SCS, conventional tonic stimulation was delivered in incremental voltages ranging from 0 to 5 V, with significantly less electrical artifact.

Statistical analysis

Results of von Frey filament thresholds and gait analysis parameters were expressed in terms of the mean and standard error. Statistical analysis of the results of the treadmill gait studies was carried out with JMP software (Version 10.0; SAS Institute, Inc., Cary, NC, USA) at a 95% confidence level. Statistical analysis of von Frey filament thresholds was performed using analysis of variance (using Matlab software, version 9.3.0.713579; MathWorks Inc., Natick, MA, USA) to test the effects of leg (ipsilateral vs. contralateral) and SCS status (on vs. off) at a 95% confidence level, both within single sheep and combining across the five sheep in the final protocol (#40014, #40015, #40016, #40021, #40022).

Results

von Frey measurements

Our preliminary data came from a total of eight sheep: one in which we transected the peroneal nerve and seven in which we performed CCI. All nerve injuries were applied to the left leg. As found in Figure 4, our preliminary data suggests that both sectioning and constricting the nerve lead to development of tactile hypersensitivity. We interpret this sensitivity as neuropathic pain due to the fact that nociceptive neurons fire at similar (60–80 mN) forces that elicit withdrawal in sheep (60–80 mN).[16,20] Figure 4A and C indicates reduced withdrawal threshold develops ~20 days and persists in the past 80–100 days after CCI. Figure 4B and D indicates pain may persist in the past 230 days and even in the past 1 year. Application of SCS appeared to return the painful affected left limb (blue) to that of the control, non-affected right side (red).

The results of the von Frey measurements for the five sheep included in the final protocol (#40014, #40015, #40016, #40021, and #40022) are presented in Table 1 and are expressed in terms of means and standard errors. Statistical analysis was performed using analysis of variance by leg (left vs. right) and SCS status (on vs. off). As seen in Figure 5, the baseline threshold of the left (affected) leg is significantly lower than the right (control) leg (252.9±37.6 vs. 361.5±32.4 g, $p=3\times10^{-8}$). Application of SCS significantly increases the withdrawal threshold of the left leg (297.5±21.5 g, $p=0.048$), but is still significantly lower than the unaffected right side, either with SCS ($p=0.0035$) or without it ($p=0.0016$). There is no significant difference

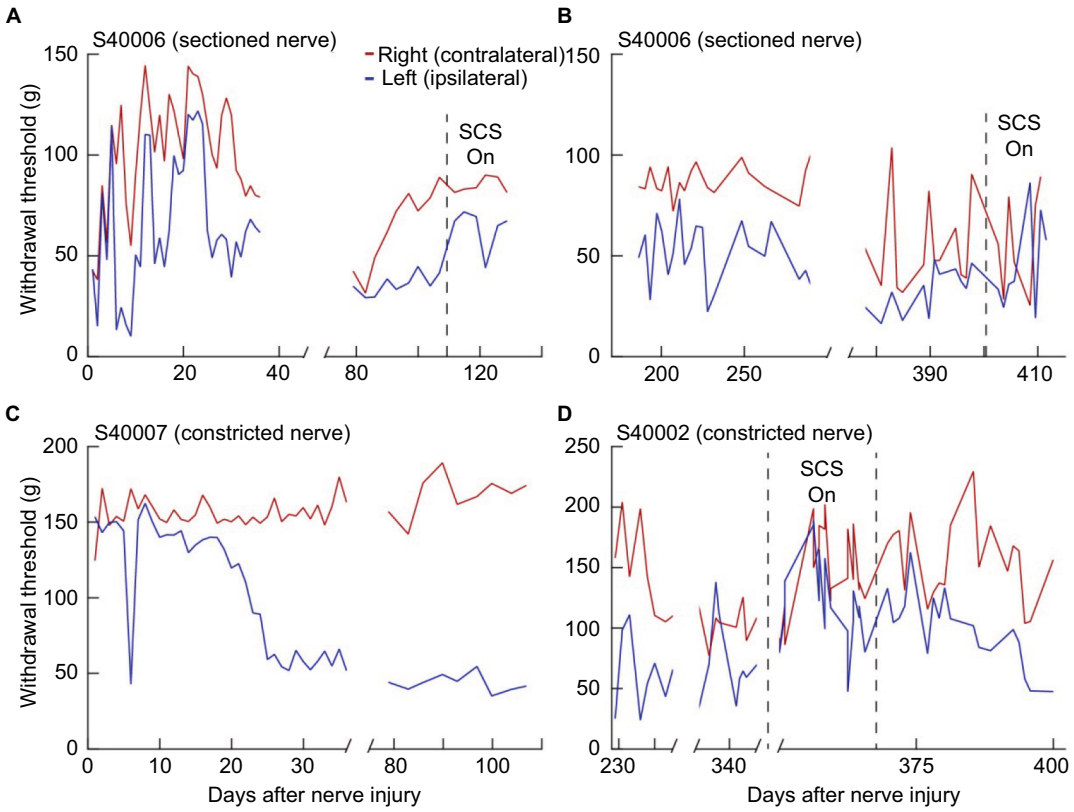

Figure 4 Withdrawal thresholds of the hind limbs in three sheep as measured with von Frey filaments and anesthesiometer from (**A, B**) one animal with a sectioned nerve and (**C, D**) two animals with constriction nerve injuries.
Notes: (**B, D**) Data collected >200 days post-nerve injury. The dashed black lines indicate portions of the data that were collected while SCS was applied continuously. The SCS appears to increase the withdrawal thresholds in the injured sheep most noticeably in (**A, D**).
Abbreviation: SCS, spinal cord stimulation.

Table 1 von Frey thresholds of five sheep in standardized protocol

Sheep	Left leg		Left leg		Right leg		Right leg	
	SCS off		SCS on		SCS off		SCS on	
	Mean (g)	±SE	Mean	±SE	Mean	±SE	Mean	±SE
40014	169.5	19.5	266.5	23.1	295.9	53.5	323.3	36.2
40015	646.4	26.6	458.1	43.6	673.3	20.7	497.9	39.6
40016	146.5	11.7	332.6	21.0	259.7	10.1	403.6	8.1
40021	194.8	16.7	232.2	28.2	353.1	24.9	324.6	13.1
40022	107.2	5.2	198.2	36.9	225.6	17.0	238.5	28.9
Mean	252.9	37.6	297.5	21.5	361.5	32.4	357.6	20.0

Abbreviation: SCS, spinal cord stimulation; SE, standard error.

in withdrawal threshold of the unaffected right side with or without SCS (357.6±20.0 vs. 361.5±32.4 g, respectively).

Treadmill data and gait analysis

Postsurgical gait

In contrast to the sheep with complete peroneal nerve transection (#40006), none of the CCI sheep developed hoof drop after surgery. By 4 weeks postoperatively, this sheep had developed a visibly compensatory gait, involving elevation of the hip to allow clearance of the hoof. Gait analysis was carried out for all sheep. Quantitative statistical analysis of the results of the treadmill gait studies was carried out with JMP software (Version 10.0; SAS Institute, Inc.) at a 95% confidence level. Auxiliary assessment methodologies included graphical inspection, evaluation of trends, and other routine practices. The two nerve injury methods had different effects on a number of parameters. For instance, the range of the flexion–extension

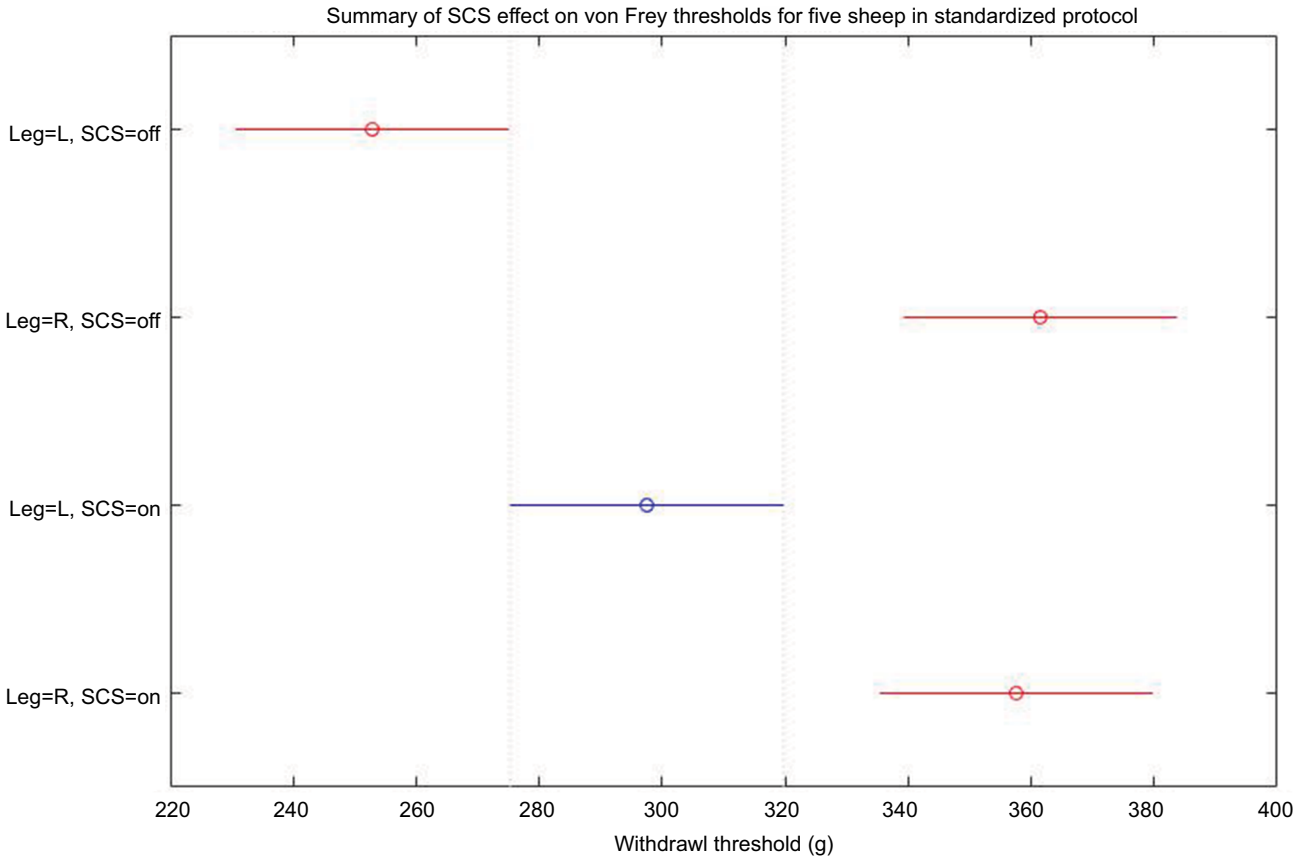

Figure 5 The results for the von Frey measurements for the five sheep included in the final protocol (#40014, #40015, #40016, #40021, and #40022) are presented in Table 1 and expressed in terms of means and standard errors.
Notes: The baseline threshold of the left (affected) leg is significantly lower than the right (control) leg (252.9±37.6 vs. 361.5±32.4 g, $p=3\times10^{-8}$). Application of SCS significantly increases the withdrawal threshold of the left leg (297.5±21.5 g, $p=0.048$), but is still significantly lower than the unaffected right side, either with SCS ($p=0.0035$) or without it ($p=0.0016$). There is no significant difference in the withdrawal threshold of the unaffected right side with or without SCS (357.6±20.0 vs. 361.5±32.4 g, respectively).
Abbreviation: SCS, spinal cord stimulation.

angle of the hock joint in the sagittal plane (referred to as the "leg swing" angle) was 63°±3.6° for the sheep with the cut peroneal nerve (#40006) and only 48°±1.1° for the animals with constricted peroneal nerves (#40002 and #40007), a relative difference of roughly 30% (Figure 6A). Moreover, the sheep with the cut peroneal nerve had an obvious motor deficit that manifested as hoof drop. After the first few weeks, it developed an altered gait pattern, in which it elevated the leg to clear the hoof. The angular speed of its contralateral (right) limb increased by ~58% in the first 100 ms of the gait cycle (Figure 6B). No such large asymmetries were observed for the leg motions of the sheep with the constricted nerves.

Effect of SCS on gait

Figure 7 demonstrates the effects of SCS on gait in the sheep with complete nerve ligation (#40006). The measurements were made on two separate days. The peak hoof elevation was 36±0.53 mm for the nerve-ligated leg during both the condition of no SCS and for stimulation at 0.1 V. At 0.3 V, the peak hoof elevations for both limbs were ~48±0.89 mm. At 0.5 V, the hoof of the ipsilateral leg was elevated to 83±2.4 mm, nearly 50% larger than the contralateral side. These results suggest that an epidural stimulation threshold exists between 0.1 and 0.3 V at which SCS allows the animal to overcome injury-induced hoof drop during normal walking. Interestingly, whereas 0.3 V brings the left hind limb to the height of the right hind limb, at 0.5 V, there appears to be a supramaximal response of both hind limbs.

Unit activity recordings

Figures 8 and 9 demonstrate the ability to obtain units and drive from the periphery, modulate them with SCS, and resolve the unit activity while simultaneously applying SCS. Typical examples of a neuron with a receptive field but no SA (Figure 8A) and a neuron firing spontaneously

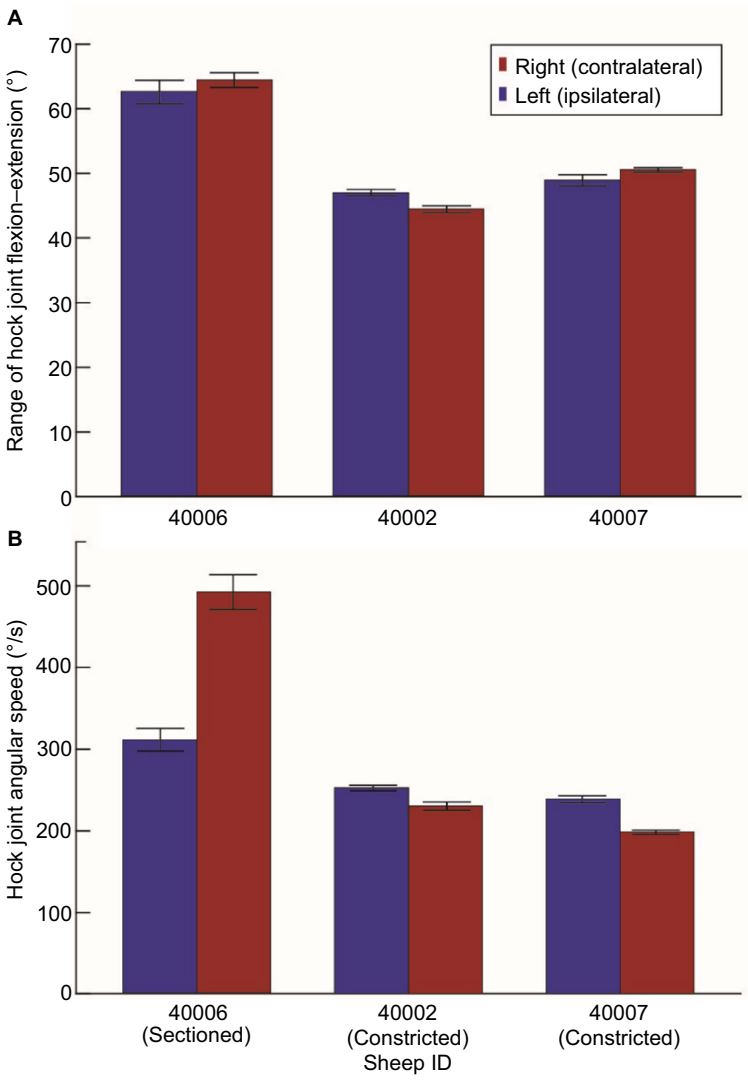

Figure 6 (**A**) Range of flexion–extension angle of the hock joint in the sagittal plane (leg swing angle). (**B**) Angular speed during the first 100 ms of the gait cycle appears to increase in the contralateral (right) limb for the sheep with the cut peroneal nerve (#40006), but this does not occur for the sheep with the constricted nerves (#40002 and #40007).
Note: Error bars represent one SD.

that also has a receptive field in the limb (Figure 8B) are shown. The firing rates of both neurons were increased with somatic stimulation. In the case of the neuron in Figure 8B, applying deep pressure to the limb increased the firing rate by ~30%.

Figure 9 shows two different examples of neuronal activity being modulated via tonic 40 Hz SCS, with the red regions indicating when SCS was applied. In both cases, the neuronal activity was successfully differentiated from the stimulus artifact, as indicated by the spike insets. At 4 and 5 V stimulation, the neuron in Figure 9A is driven, matching the 40 Hz stimulus during the 5 V stimulation. The raster plots, aligned to each stimulus artifact, show the neuron becoming more tightly driven by the stimulus at higher intensities. The neuron in Figure 9B displays the opposite behavior as in Figure 9A, becoming suppressed at higher stimulation intensities. The inset from the 3 V region shows the complete absence of spikes during the SCS.

Discussion

Significance of the ovine model

Newer modalities of SCS, namely, high-frequency and burst, afford superior clinical relief from back and leg pain compared to conventional tonic SCS, without the paresthesias seen in tonic SCS. Despite excellent clinical evidence in support of these new modalities,[4,5] the basic mechanisms underlying the relative superiority of the newer paresthesia-free modalities relative to conventional SCS are less well understood.[6] Much

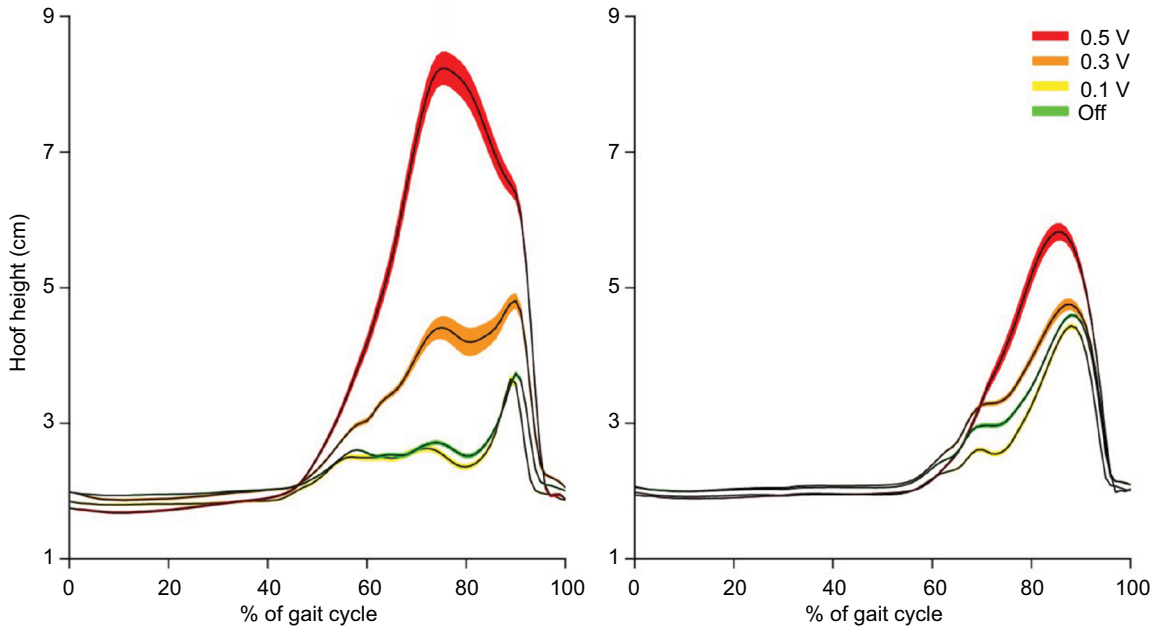

Figure 7 Mean height of both back hooves plotted against percent of gait cycle for the sheep with a cut peroneal nerve (#40006).
Notes: Each trace is the average of 120–130 steps time-normalized to the gait cycle percentage. No difference in height is seen in the nerve-injured (ipsilateral) limb for SCS at 0 V (off) and 0.1 V, but significant increases in hoof elevation are seen during SCS at 0.3 and 0.5 V. The mean contralateral hoof elevation remains mostly constant from SCS off to 0.3 V and increases with 0.5 V stimulation. Shaded error bars represent standard error.
Abbreviation: SCS, spinal cord stimulation.

of the scientific support for the mechanisms underlying SCS is derived from small animal models[2,9] and computer modeling.[35] To date, however, there is no large animal model of neuropathic pain which has been utilized to test both acute and chronic mechanistic effects of SCS, with both behavioral and electrophysiologic endpoints. From an overall qualitative perspective, and as discussed in detail below, the useful outcomes from this exploratory version of our model include the following findings: 1) we have introduced a large animal implementation with the significant advantage that the motor system is spared compared with previous models; 2) we have demonstrated successful implantation and use of SCS and single-unit recordings with minimal impact of artifacts, thus pointing the way toward possible experimental elucidation of mechanisms of action underlying SCS; and 3) we have demonstrated the feasibility of employing this model to assess pain thresholds and the workability of gait analysis to explore potential responses to therapies.

Our large animal ovine model affords several advantages. The similar size of the sheep spinal cord to the human spinal cord[36] allows testing of large clinical grade SCS hardware in both the acute and chronic settings. The larger size of the spinal cord relative to rodent models allows simultaneous stimulation and recording, with minimal electrical artifact, which is often not possible in a smaller animal model.[7]

Our model is based on a previous ovine model of neuropathic pain, in which the nerve was sectioned.[16] Unlike the previous model, however, we adapt a CCI, more commonly used in rodents,[22,37] in order to avoid a motor deficit of hoof drop, creating a state of neuropathic pain more similar to the typical clinical manifestation. For these reasons, our model may be useful in exploring mechanistic questions regarding the effect of SCS on both behavior and electrophysiology. We note, however, that while motor deficits such as hoof drop were not observed over the duration of our study's protocol, the possibility may exist for emergence of such effects at later times.[53]

Better understanding of the mechanisms underlying pain relief produced by all modes of SCS has significant clinical and financial implications. Development of a large animal model of neuropathic pain which is capable of accommodating clinical grade SCS devices also provides a test bed for newer technology and modes of stimulation.[38]

Potential of the model for investigating mechanisms of SCS

Current underlying theory regarding the mechanism of conventional SCS is rooted in the "Gate Theory of Pain".[39] With modifications over time,[2] the preponderance of data suggests that activation of the dorsal columns leads to suppression of WDR neurons in the dorsal horn via inhibitory GABA-ergic

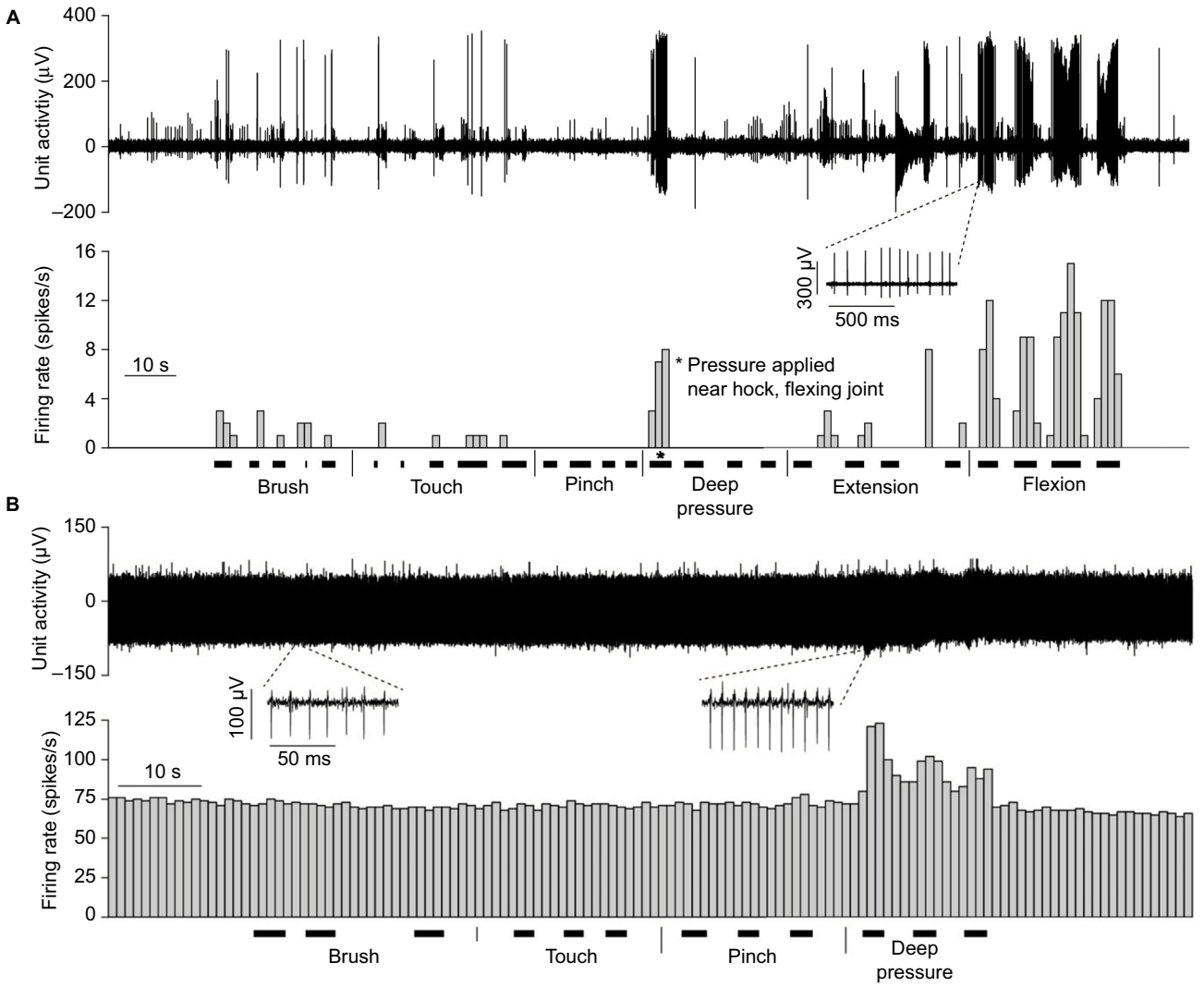

Figure 8 Example recordings of dorsal horn neurons (**A**) without spontaneous activity and (**B**) with spontaneous activity.
Notes: Both neurons were recorded from the same sheep (#40015) with a CCI. Neuronal responses to various stimuli, including brushing, touching, pinching, and applying deep pressure to the gastrocnemius muscle and flexion and extension of the hock joint, are shown. The upper and lower panels show the digitized raw action potentials and the neuron's firing rate (cumulative histogram, bin width=1 s), respectively.
Abbreviation: CCI, chronic constriction injury.

interneurons. This is based on animal work and the corresponding clinical observation that paresthesias in the distribution of pain are required for eliminating pain.[40] Without paresthesias, tonic SCS does not work, so much so that most trialing procedures are done under minimal sedation, in order to test adequately if the patient has matching paresthesias in the distribution of pain.

With the advent of high-frequency and burst stimulation, different mechanisms of pain relief were proposed. The patients in tests of these modalities did not feel paresthesias and were not required to remain awake during SCS trials. Unlike the optimal location of T8/9 in traditional SCS, these patients were targeted for T9/10, suggesting a direct action in the dorsal horn at the segmental levels responsible for back and leg pain (T11–L2) vs. an indirect mechanism mediated via the dorsal columns. Recent modeling[35] suggests increased frequency of stimulation may set an increased electric field in the dorsal horn, hyperpolarizing the cells inside and inhibiting pain transmission. This may be a frequency-dependent rather than a charge-dependent effect.[6]

However, a contrasting school of thought contends that the efficacy of high-frequency (HF10) stimulation is not a frequency-dependent phenomenon, but instead a charge-dependent or "duty cycle" phenomenon.[6] We have recently observed clinically that some patients with "high-density" programs found good pain relief, and many were without

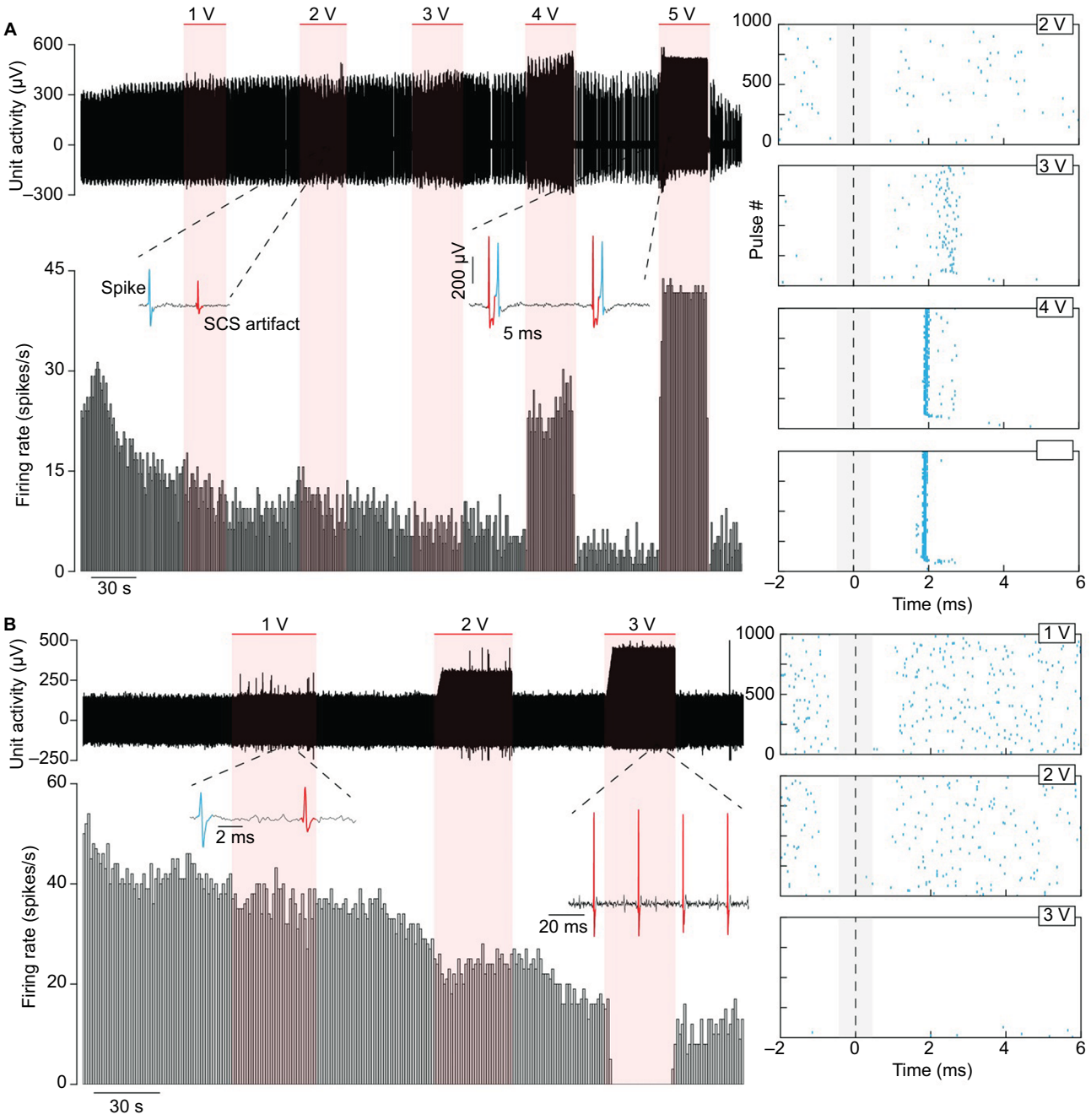

Figure 9 Neuronal activity of two neurons from different blocks recorded during SCS from the same sheep (#40022).

Notes: (**A**) One neuron was excited by SCS and (**B**) the other neuron inhibited. The horizontal red bars indicate the regions where 40 Hz SCS was applied at varying amplitudes. Below the raw waveform in each panel is the neuron's firing rate (cumulative histogram, bin width=1 s). The raster plots show the neurons' action potentials aligned to each individual pulse of the SCS. The neuron in (**A**) is driven by the SCS above 3 V with a latency of ~2 ms. In (**B**), the neuron is completely suppressed with SCS at 3 V.

Abbreviation: SCS, spinal cord stimulation.

paresthesias, supporting the claim that paresthesia freedom may not be a frequency-dependent phenomenon, but a charge-dependent phenomenon.[41]

Our work demonstrates the feasibility of developing a sheep neuropathic pain model to test the behavioral and electrophysiologic effects of acute and chronic SCS and to begin exploring the mechanisms responsible for its effects. This set of studies adds to the extant body of literature in several ways.

First, CCI of the peroneal nerve effectively produces tactile hypersensitivity in the absence of the foot drop seen in nerve transection models. While motor deficits were observed in the sheep with the transected nerve, neither direct observation nor gait analysis revealed any gross motor deficits in

CCI sheep. To our knowledge, this is the first ovine model of neuropathic pain utilizing the CCI. We interpret tactile hypersensitivity to be a surrogate for pain based on the observations that specific nociceptive neurons are activated at 80 mN[20] and the withdrawal threshold in normal sheep is >60 mN.[16]

Second, a dorsal horn recording apparatus similar to that described by Herrero et al[19] was constructed for the purpose of reliably obtaining high-quality recordings of DHN activity. While recording from the dorsal horn, the electrical SCS artifact could be identified and removed, allowing analysis of dorsal horn activity during SCS. The externalized stimulator allowed for the application of novel high-frequency and burst waveforms.[6,35] Understanding the therapeutic mechanisms of these newer waveforms is of timely clinical importance as these options have now become clinically available for patient populations.[5,9,38,42]

Third, the effects of SCS on von Frey filament thresholds demonstrate a reversal of the tactile hypersensitivity developing after nerve injury. SCS also ameliorated the gross gait abnormalities produced by nerve injury. However, we do not know if SCS was mitigating tactile hypersensitivity or introducing or modifying any motor effects. Mitigation of tactile hypersensitivity was evidenced by an increase in von Frey threshold of the affected limb at a continuous stimulation setting of 0.1 V. Motor changes in gait were noted at higher voltages, suggesting lower voltages affected the sensory function with higher voltages affecting the motor function, but this merits further study. We also note that in addition to serving as a useful model for testing fully implanted clinical grade systems, other work in our laboratories[43–45] has shown that the adult sheep is well suited for evaluating the performance characteristics of a novel type of intradural spinal cord stimulator now under development.[36,46–49]

The small number of animals included in the principal part of this pilot study, along with foregoing of animals representing sham interventions, hampers the generalizability of our results. In particular, this limits what we can conclude about the impact of SCS on the behavioral findings. However, the preliminary evidence does suggest that SCS can modulate both neuronal physiology and gross behavior in an ovine model of nerve injury. This outcome is in keeping with recent reports of similar sensorimotor effects produced by epidural electrical stimulation in small animals.[50]

Lastly, we note the recent comparison of low-frequency ("tonic") to high-frequency ("kilohertz") stimulation paradigms,[41] the latter of which may provide improved pain relief for patients, as might burst-mode approaches.[34] We further note that high-frequency stimulation has been assessed at the level of the peripheral nerve to block the transmission of pain signals.[51,52] All these emphasize the potential utility of developing a model that will enable studies of electrophysiologic responses to stimulation methodologies and parameters. The hope is that such knowledge can be extended to develop novel stimulation paradigms and devices for patients with chronic neuropathic pain. The ovine model shows promise of helping to bridge the gap between small animal models and improved patient care.

Conclusion

Sheep with a chronically constricted peroneal nerve develop a neuropathic pain syndrome over the course of 2–3 weeks, without detectable motor deficit. SCS appears to reverse mechanical hypersensitivity to near-baseline levels, presumably alleviating nociception. These studies demonstrate the feasibility of applying chronic SCS in nerve-injured sheep during treadmill gait analysis. Furthermore, this large animal model permits dorsal horn unit activity recording in the presence and absence of active SCS. In additional to conventional tonic SCS, novel paradigms of burst and high-frequency stimulation can be applied, while simultaneously measuring dorsal horn activity. Taken together, this model provides an ideal arrangement for assessing the mechanisms underlying the effects of SCS.

This body of work demonstrates the feasibility of developing a large animal (ovine) neuropathic pain model for the purpose of testing the mechanisms and effects of acute and chronic SCS on behavioral measures of von Frey filament thresholds and gait analysis, as well as electrophysiologic measures during DHN recordings.

Acknowledgments

The authors thank University of Iowa colleagues ND Jeffery, TL Weaver, E Petersen, A Malandra, A Parrish, H Chen, S Viljoen, KN Gibson-Corley, NM Grosland, NU Jerath, K Stoner, R Reale, F Jareczek, and H Kawasaki for technical assistance and useful discussions. They also thank the Iowa State University colleagues SK Shivapour, T Zylstra, and Mahdi Zamanighomi for assistance with the gait analysis.

Disclosure

The authors report no conflicts of interest in this work.

References

1. Pizzo PA, Clark NM, Carter-Pokras O, et al. *Institutes of Medicine: Relieving Pain in America: A Blueprint for Transforming Prevention, Care, Education, and Research*. Washington, DC: The National Academies Press; 2011.

2. Foreman RD, Linderoth B. Neural mechanisms of spinal cord stimulation. *Int Rev Neurobiol*. 2012;107:87–119.
3. Kumar K, Taylor RS, Jacques L, et al. The effects of spinal cord stimulation in neuropathic pain are sustained: a 24-month follow-up of the prospective randomized controlled multicenter trial of the effectiveness of spinal cord stimulation. *Neurosurgery*. 2008;63(4):762–770; discussion 770.
4. Kapural L, Yu C, Doust MW, et al. Novel 10-kHz high-frequency therapy (HF10 therapy) is superior to traditional low-frequency spinal cord stimulation for the treatment of chronic back and leg pain: the SENZA-RCT randomized controlled trial. *Anesthesiology*. 2015;123(4):851–860.
5. Hou S, Kemp K, Grabois M. A Systematic evaluation of burst spinal cord stimulation for chronic back and limb pain. *Neuromodulation.* 2016;19(4):398–405.
6. Miller JP, Eldabe S, Buchser E, Johanek LM, Guan Y, Linderoth B. Parameters of spinal cord stimulation and their role in electrical charge delivery: a review. *Neuromodulation.* 2016;19(4):373–384.
7. Guan Y, Wacnik PW, Yang F, et al. Spinal cord stimulation-induced analgesia: electrical stimulation of dorsal column and dorsal roots attenuates dorsal horn neuronal excitability in neuropathic rats. *Anesthesiology*. 2010;113(6):1392–1405.
8. Shechter R, Yang F, Xu Q, et al. Conventional and kilohertz-frequency spinal cord stimulation produces intensity- and frequency-dependent inhibition of mechanical hypersensitivity in a rat model of neuropathic pain. *Anesthesiology*. 2013;119(2):422–432.
9. Tang R, Martinez M, Goodman-Keiser M, Farber JP, Qin C, Foreman RD. Comparison of burst and tonic spinal cord stimulation on spinal neural processing in an animal model. *Neuromodulation.* 2014;17(2):143–151.
10. Yang F, Xu Q, Cheong YK, et al. Comparison of intensity-dependent inhibition of spinal wide-dynamic range neurons by dorsal column and peripheral nerve stimulation in a rat model of neuropathic pain. *Eur J Pain*. 2014;18(7):978–988.
11. Balasubramanyan S, Stemkowski PL, Stebbing MJ, Smith PA. Sciatic chronic constriction injury produces cell-type-specific changes in the electrophysiological properties of rat substantia gelatinosa neurons. *J Neurophysiol*. 2006;96(2):579–590.
12. Chen Y, Balasubramanyan S, Lai AY, Todd KG, Smith PA. Effects of sciatic nerve axotomy on excitatory synaptic transmission in rat substantia gelatinosa. *J Neurophysiol*. 2009;102(6):3203–3215.
13. Devor M. Centralization, central sensitization and neuropathic pain. Focus on "sciatic chronic constriction injury produces cell-type-specific changes in the electrophysiological properties of rat substantia gelatinosa neurons". *J Neurophysiol.* 2006;96(2):522–523.
14. Laird JM, Bennett GJ. An electrophysiological study of dorsal horn neurons in the spinal cord of rats with an experimental peripheral neuropathy. *J Neurophysiol.* 1993;69(6):2072–2085.
15. Sandkuhler J. Models and mechanisms of hyperalgesia and allodynia. *Physiol Rev*. 2009;89(2):707–758.
16. Wilkes D, Li G, Angeles CF, Patterson JT, Huang LY. A large animal neuropathic pain model in sheep: a strategy for improving the predictability of preclinical models for therapeutic development. *J Pain Res*. 2012;5:415–424.
17. Butt M, Alataris K, Walker A, Tiede J. F702 histological findings using novel stimulation parameters in a caprine model. *Eur J Pain Suppl*. 2011;5(S1):188–189.
18. Castel D, Sabbag I, Brenner O, Meilin S. Peripheral neuritis trauma in pigs: a neuropathic pain model. *J Pain.* 2016;17(1):36–49.
19. Herrero JF, Coates TW, Higgins M, Livingston A, Waterman AE, Headley PM. A technique for recording from spinal neurones in awake sheep. *J Neurosci Methods*. 1993;46(3):225–232.
20. Herrero JF, Headley PM. Cutaneous responsiveness of lumbar spinal neurons in awake and halothane-anesthetized sheep. *J Neurophysiol*. 1995;74(4):1549–1562.
21. Bennett GJ, Chung JM, Honore M, Seltzer Z. Models of neuropathic pain in the rat. *Curr Protoc Neurosci*. 2003;Chapter 9:Unit 9.14.
22. Bennett GJ, Xie YK. A peripheral mononeuropathy in rat that produces disorders of pain sensation like those seen in man. *Pain*. 1988;33(1):87–107.
23. Shortland P, Kinman E, Molander C. Sprouting of A-fibre primary afferents into lamina II in two rat models of neuropathic pain. *Eur J Pain*. 1997;1(3):215–227.
24. Ley SJ, Livingston A, Waterman AE. The effect of chronic clinical pain on thermal and mechanical thresholds in sheep. *Pain*. 1989;39(3):353–357.
25. Nolan A, Livingston A, Morris R, Waterman A. Techniques for comparison of thermal and mechanical nociceptive stimuli in the sheep. *J Pharmacol Methods*. 1987;17(1):39–49.
26. Stubsjoen SM, Flo AS, Moe RO, et al. Exploring non-invasive methods to assess pain in sheep. *Physiol Behav*. 2009;98(5):640–648.
27. Welsh EM, Nolan AM. Effect of flunixin meglumine on the thresholds to mechanical stimulation in healthy and lame sheep. *Res Vet Sci*. 1995;58(1):61–66.
28. Hamilton L, Franklin RJ, Jeffery ND. Development of a universal measure of quadrupedal forelimb-hindlimb coordination using digital motion capture and computerised analysis. *BMC Neurosci*. 2007;8:77.
29. Hamilton L, Franklin RJ, Jeffery ND. Quantification of deficits in lateral paw positioning after spinal cord injury in dogs. *BMC Vet Res*. 2008;4:47.
30. Safayi S, Miller JW, Wilson S, et al. Treadmill measures of ambulation rates in ovine models of spinal cord injury and neuropathic pain. *J Med Eng Technol*. 2016;40(3):72–79.
31. Safayi S, Jeffery ND, Fredericks DC, et al. Biomechanical performance of an ovine model of intradural spinal cord stimulation. *J Med Eng Technol*. 2014;38(5):269–273.
32. Safayi S, Jeffery ND, Shivapour SK, et al. Kinematic analysis of the gait of adult sheep during treadmill locomotion: parameter values, allowable total error, and potential for use in evaluating spinal cord injury. *J Neurol Sci*. 2015;358(1–2):107–112.
33. Zahn PK, Brennan TJ. Incision-induced changes in receptive field properties of rat dorsal horn neurons. *Anesthesiology*. 1999;91(3):772–785.
34. De Ridder D, Vanneste S, Plazier M, van der Loo E, Menovsky T. Burst spinal cord stimulation: toward paresthesia-free pain suppression. *Neurosurgery*. 2010;66(5):986–990.
35. Arle JE, Mei L, Carlson KW, Shils JL. High-frequency stimulation of dorsal column axons: potential underlying mechanism of paresthesia-free neuropathic pain relief. *Neuromodulation*. 2016;19(4):385–397.
36. Viljoen S, Dalm BD, Reddy CG, et al. Optimization of intradural spinal cord stimulation designs via analysis of thoracic spine imaging data. *J Med Biol Eng*. 2013;33(2):193–198.
37. Dalm BD, Reddy CG, Howard MA, Kang S, Brennan TJ. Conditioned place preference and spontaneous dorsal horn neuron activity in chronic constriction injury model in rats. *Pain*. 2015;156(12):2562–2571.
38. De Ridder D, Vanneste S. Visions on the future of medical devices in spinal cord stimulation: what medical device is needed? *Expert Rev Med Devices*. 2016;13(3):233–242.
39. Melzack R, Wall PD. Pain mechanisms: a new theory. *Science*. 1965;150(3699):971–979.
40. North RB, Streelman K, Rowland L, Foreman PJ. Spinal cord stimulation paresthesia and activity of primary afferents. *J Neurosurg Spine*. 2012;17(4):363–366.
41. Reddy CG, Dalm BD, Flouty OE, Gillies GT, Howard MA 3rd, Brennan TJ. Comparison of conventional and kilohertz frequency epidural stimulation in patients undergoing trialing for spinal cord stimulation: clinical considerations. *World Neurosurg*. 2016;88:586–591.
42. Kriek N, Groeneweg JG, Stronks DL, Huygen FJ. Comparison of tonic spinal cord stimulation, high-frequency and burst stimulation in patients with complex regional pain syndrome: a double-blind, randomised placebo controlled trial. *BMC Musculoskelet Disord*. 2015;16:222.

43. Dalm BD, Viljoen SV, Dahdaleh NS, et al. Revisiting intradural spinal cord stimulation: an introduction to a novel intradural spinal cord stimulation device. *Innov Neurosurg.* 2014;2(1–4):13–20.
44. Huang Q, Oya H, Flouty OE, et al. Comparison of spinal cord stimulation profiles from intra- and extradural electrode arrangements by finite element modelling. *Med Biol Eng Comput*. 2014;52(6):531–538.
45. Oya H, Safayi S, Jeffery ND, et al. Soft-coupling suspension system for an intradural spinal cord stimulator: biophysical performance characteristics. *J Appl Phys*. 2013;114(16):164701.
46. Gibson-Corley KN, Flouty O, Oya H, Gillies GT, Howard MA. Post-surgical pathologies associated with intradural electrical stimulation in the central nervous system: design implications for a new clinical device. *BioMed Res Int*. 2014;2014:989175.
47. Howard MA, Utz M, Brennan TJ, et al. Intradural approach to selective stimulation in the spinal cord for treatment of intractable pain: design principles and wireless protocol. *J Appl Phys*. 2011;110(4):044702.
48. Oliynyk MS, Gillies GT, Oya H, Wilson S, Reddy CG, Howard MA. Dynamic loading characteristics of an intradural spinal cord stimulator. *J Appl Phys*. 2013;113(2):026103.
49. Viljoen S, Smittkamp CA, Dalm BD, et al. MR-based measurement of spinal cord motion during flexion of the spine: implications for intradural spinal cord stimulator systems. *J Med Eng Technol.* 2014;38(1):1–4.
50. Wenger N, Moraud EM, Raspopovic S, et al. Closed-loop neuromodulation of spinal sensorimotor circuits controls refined locomotion after complete spinal cord injury. *Sci Transl Med*. 2014;6(255):255ra133.
51. Ackermann DM Jr, Bhadra N, Foldes EL, Kilgore KL. Conduction block of whole nerve without onset firing using combined high frequency and direct current. *Med Biol Eng Comput*. 2011;49(2):241–251.
52. Joseph L, Butera RJ. High-frequency stimulation selectively blocks different types of fibers in frog sciatic nerve. *IEEE Trans Neural Syst Rehabil Eng*. 2011;19(5):550–557.
53. Bagriyanik HA, Ersoy N, Cetinkaya C, et al. The effects on chronic constriction injury of sciatic nerve in rats. *Neurosci Lett*. 2014;561:123–127.